

# Recovery from liver disease in a Niemann-Pick type C mouse model

Naomi L. Sayre,\* Victoria M. Rimkunas,\* Mark J. Graham,<sup>†</sup> Rosanne M. Crooke,<sup>†</sup> and Laura Liscum<sup>1,\*</sup>

Department of Physiology,\* Tufts University School of Medicine, 136 Harrison Avenue, Boston, MA 02111; and Cardiovascular Disease Antisense Drug Discovery,<sup>†</sup> Isis Pharmaceuticals, Inc., 1896 Rutherford Road, Carlsbad, CA 92008

**Abstract** Loss of function of Niemann-Pick C1 (NPC1) leads to lysosomal free cholesterol storage, resulting in the neurodegenerative disease Niemann-Pick disease type C (NPC). Significant numbers of patients with NPC also suffer from liver disease. Currently, no treatments exist that alter patient outcome, and it is unknown if recovery from tissue damage can occur even if a treatment were found. Our laboratory developed a strategy to test whether mice can recover from NPC liver disease. We used antisense oligonucleotides to knock down hepatic expression of NPC1 in BALB/C mice for either 9 or 15 weeks. This recapitulated liver disease with hepatomegaly, cell death, and fibrosis. Then, antisense oligonucleotide treatment was halted for an additional 4, 9, or 15 weeks. We report that significant liver recovery occurred even when NPC1 protein expression only partially returned to normal. Several pathological phenotypes were alleviated, including hepatomegaly, cholesterol storage, and liver cell death. Histological examination revealed that foamy cell accumulation was relieved; however, liver fibrosis increased. Additionally, resolution of cholesterol storage and liver cell death took longer in mice with long-term knockdown. Finally, we found that transcription of cholesterol homeostatic genes was significantly disrupted during the recovery phase after long-term knockdown.—Sayre, N. L., V. M. Rimkunas, M. J. Graham, R. M. Crooke, and L. Liscum. **Recovery from liver disease in a Niemann-Pick type C mouse model.** *J. Lipid Res.* 2010. 51: 2372–2383.

**Supplementary key words** lysosomal storage disease • sterol responsive element binding protein-2 • liver X receptor • HMG CoA reductase • ATP-binding cassette G5

The fatal neurodegenerative disease Niemann-Pick type C (NPC) is caused by loss of function of NPC1 in 95% of

clinical cases and NPC2 in 5% of clinical cases. NPC is characterized by storage of free cholesterol and glycosphingolipids in late endosomes and lysosomes. The clinical phenotype that arises, neurodegeneration, hepatosplenomegaly, ataxia, seizures, and dystonia, is similar regardless of whether NPC1 or NPC2 is the cause (1).

Although most NPC patients die due to complications of their neurodegenerative disease, some patients also develop liver disease. Aside from hepatosplenomegaly, NPC patients often suffer from prolonged neonatal jaundice and ascites (2), as well as liver failure (3–7). NPC is the second most common cause of neonatal cholestasis (7), and 10% of these patients die because of liver failure (8). On the tissue level, livers from NPC-diseased mice exhibit increased hepatocyte apoptosis, infiltration of foamy macrophages, inflammation, proliferation of hepatic stellate cells, and fibrosis (9–11). To better understand liver disease in NPC, our laboratory has developed a mouse model using 2'-O-methoxyethyl modified antisense oligonucleotides (ASO) to block expression of NPC1 specifically in the liver (10).

In the present study, we aimed to determine whether recovery is possible in mice with NPC-associated liver disease by using ASOs to knock down hepatic NPC1 expression. After halting treatment for different lengths of time, liver disease was assessed. We hypothesized that extensive liver recovery was possible in NPC1 ASO-treated mice, because the liver has a remarkable capacity for regeneration (12). Here, we show that substantial reversal of the NPC disease phenotype occurred, including alleviation of hepatomegaly, loss of lipid-laden macrophage accumulations, and decreasing liver cell apoptosis. Much pathology

Abbreviations: ABCG5, ATP-binding cassette G5; ALT, alanine aminotransferase; ASO, antisense oligonucleotide; BrdU, bromodeoxyuridine; H/E, hematoxylin and eosin; HMG, 3-hydroxy-3-methylglutaryl; HSD, honestly significant difference; LXR, liver X receptor; NPC, Niemann-Pick disease type C; NPC1, Niemann-Pick C1; MM, mismatched; QPCR, quantitative PCR; SREBP2, sterol responsive element binding protein 2; TBS/T, TBS containing 1% Tween-20; TUNEL, terminal deoxynucleotidyl transferase dUTP nick end labeling.

<sup>1</sup>To whom correspondence should be addressed.  
e-mail: laura.liscum@tufts.edu

This work was supported by National Institutes of Health Grants R01 DK-49564 and T32 DK-07542, and by the Tufts Center for Neurosciences Research P30 NS047243. Its contents are solely the responsibility of the authors and do not necessarily represent the official views of the National Institutes of Health or other granting agencies.

Manuscript received 29 March 2010 and in revised form 24 April 2010.

Published, JLR Papers in Press, April 24, 2010  
DOI 10.1194/jlr.M007211

resolved even with partial expression of NPC1 protein. Despite significant recovery, liver fibrosis increased over time and, in 15 week NPC1 ASO-treated mice, cholesterol homeostasis was disrupted.

## EXPERIMENTAL PROCEDURES

### Oligonucleotides

The 20-mer 2'-*O*-methoxyethyl-modified ASOs were synthesized and purified as described previously (13, 14). Two sequences were used: one was targeted to NPC1 mRNA (5'CCCGATTGAGCTCATCTTCG3'), and as a control, a second ASO with a mismatched sequence was used that has no mRNA target (5'CCTTCCCTGAAGGTTCCCTCC3'). ASOs were dissolved in 0.9% saline and stored at -20°C until use.

### Animal care and treatment

All procedures were approved by the Institutional Animal Care and Use Committee at Tufts University and were in compliance with the National Institutes of Health Guide for the Care and Use of Laboratory Animals. Four-week-old female BALB/c mice were purchased from the Jackson Laboratory (Bar Harbor, ME). Mice were housed up to five animals per cage and fed rodent chow. Twice weekly, mice were injected intraperitoneally with either NPC1 ASO or mismatched control ASO at a dose of 50 mg/kg of body weight for either 9 or 15 weeks. After treatment, mice were either euthanized or allowed to recover for additional 4, 9, or 15 weeks. Mice were then fasted overnight and euthanized. Blood samples were taken via cardiac puncture, and then mice were perfused with an ice-cold solution of PBS containing protease inhibitor cocktail tablets (Roche, Nutley, NJ; 2 tablets/50 ml), phosphatase inhibitor cocktail 2 (Sigma, Woodstock, VA; 300 µl/50 ml), and 5 mM sodium fluoride. After perfusion, tissue samples were dissected and taken for paraffin-embedded histology by fixing in 10% formalin or were snap-frozen in liquid nitrogen.

### Tissue homogenization

For SDS-PAGE and Western blotting, liver tissue was manually homogenized using a mini-mortar and pestle in ice-cold 1% Nonidet P-40 lysis buffer [20 mM Tris-HCl, pH 8, 137 mM NaCl, 10% glycerol, 1% NP-40, 2 mM EDTA, protease inhibitor cocktail tablets (1 tablet/20 ml buffer), phosphatase inhibitor cocktail 2 (200 µl/20 ml buffer), 10 mM NaF] and then sonicated at 2 volts for a period of 10 s. Samples were centrifuged at 2,500 *g* for 10 min. For cholesterol content analysis, liver tissue was manually homogenized in cold-saline and sonicated at 2 volts for 10 s. Protein concentrations were determined using the bicinchoninic acid protein assay kit (Pierce, Rockford, IL).

### Western blotting of NPC1

Protein lysates were subjected to SDS-PAGE using the Invitrogen Novex mini-gel system. Lysates (25 µg) were diluted in 6× reducing Laemmli's SDS-Sample Buffer (Boston BioProducts, Worcester, MA), incubated for 1 min at 60°C, and run on 10% Bis-Tris mini-gels (Invitrogen, Carlsbad, CA) in MOPS running buffer (50 mM MOPS, 50 mM Tris base, 0.1% SDS, 1 mM EDTA; pH 7.7). Proteins were transferred onto 0.2 µm nitrocellulose according to the manufacturer's instructions. Membranes were blocked in 5% nonfat milk in TBS containing 1% Tween-20 (TBS/T) and then incubated overnight at 4°C with a 1:1,000 dilution of anti-NPC1 (Abcam, Cambridge, MA) or 1:15,000 dilution of anti-β-actin (Sigma, Woodstock, VA). Membranes were rinsed four times for 15 min each time in TBS/T, and then probed with a 1:1,000 dilu-

tion of species-specific horseradish peroxidase-conjugated secondary antibody (Sigma, Woodstock, VA) for 1 h at room temperature. Membranes were rinsed 4 times for 15 min each time in TBS/T and developed using Western Lightning-ECL reagent (Perkin-Elmer, Boston, MA) according to the manufacturer's instructions. Relative amounts of liver NPC1 protein expression were determined with densitometry using Image-J software. Protein expression was normalized to β-actin in all samples.

### Serum chemistries

Blood was allowed to clot for 20–30 min in Serum Separator Tubes (Becton, Dickinson, San Jose, CA) and then centrifuged at 740 *g* for 30 min to separate the plasma from cellular blood matter. Serum chemistries were determined by Idexx Laboratories (Grafton, MA).

### RNA harvest and first-strand DNA synthesis

Fresh or snap-frozen liver tissue (25–50 mg) was homogenized in 500 µl Trizol (Invitrogen, Carlsbad, CA), and total RNA was harvested according to the manufacturer's instructions. RNA concentration was determined by measuring absorbance at 260 nm, and integrity of RNA was verified by visualizing intact 18S and 28S rRNA on an agarose gel before first-strand DNA synthesis. RNA was stored at -80°C until use.

To synthesize first-strand DNA, the SuperScript III First-Strand Synthesis Supermix (Invitrogen, Carlsbad, CA) was used according to the manufacturer's instructions. First-strand DNA was stored at -20°C until use for quantitative PCR (QPCR).

### QPCR

To perform QPCR, first-strand DNA, primers, and Brilliant II SYBR Green QPCR master mix (Stratagene, Cedar Creek, TX) were mixed together. The reactions were incubated on a Stratagene MX4000 thermocycler, and gene expression was normalized using glyceraldehyde 3-phosphate dehydrogenase and then analyzed by the comparative C<sub>T</sub> method. RNA levels are expressed relative to values obtained from mismatched ASO-treated mice. Values are reported as averages from triplicate reactions, and SDs reflect variability of 3–5 mice/treatment group.

Primers used were previously designed and are shown 5' to 3': *procollagen Iα2* (Genbank NM\_007743) (15) F: CTC CAA GGA AAT GGC AAC TCA G, R: TCC TCA TCC AGG TAC GCA ATG; *SREBP2* (Genbank NM\_033218) (16) F: ACA AAC TTG CTC TGA AAA CAA ATC, R: GCG TTC TGG AGA CCA TGG A; *3-hydroxy-3-methylglutaryl CoA reductase* (Genbank NM\_008255) (17) F: CTT GTG GAA TGC CTT GTG ATT G, R: AGC CGA AGC AGC ACA TGA T; *LXR-α* (Genbank NM\_013839) (18) F: AGG AGT GTC GAC TTC GCA AA, R: CTC TTC TTG CCG CTT CAG TTT; *ABCG5* (Genbank NM\_031884) (17) F: TGG ATC CAA CAC CTC TAT GCT AAA, R: GGC AGG TTT TCT CGA TGA ACT G.

### Measurement of cholesterol content

Lysates (200–300 µg) of tissues homogenized in saline were subjected to Folch extraction (19). As an internal standard, 45 µg of stigmasterol was added to each sample before extraction. To measure free cholesterol, isolates from the Folch organic phase were injected into a Hewlett-Packard 5890 gas chromatograph with a DB-17 column (15m × 0.53 mm, Alltech) at 255°C.

To measure total cholesterol (free plus esterified cholesterol), the Folch organic phase was subjected to saponification (20). Isolates from the Folch organic phase were diluted in 1 ml of 50% ethanol, and cholesteryl esters were hydrolyzed to free cholesterol by treating with 1 ml 1M KOH in 95% ethanol at 80°C for 1 h. The free cholesterol was extracted using petroleum ether and then backwashed with distilled water. Isolates from the organic-phase

of the petroleum ether extraction were injected into the gas chromatograph. Cholesteryl ester content was determined by subtracting free cholesterol measurements from total cholesterol measurements for each sample. Reported values represent averages from two separate extractions, and SDs reflect variability of 5–6 mice/treatment group.

### Histology

Fixed liver tissue was paraffin-embedded, and 5  $\mu$ m sections were taken. Sections were stained with hematoxylin/eosin (H/E) or Masson Trichrome by the Tufts Animal Histology Core or the Tufts Medical Center Histology Department, respectively. For all tests, 10 random fields were used for quantification per animal. Reported values are expressed as averages with SDs from 3–6 animals per treatment group.

The numbers of hepatocytes and lipid-laden cells were determined by quantifying the number of cells per field at 200 $\times$  magnification. The amount of fibrosis was determined by manually replacing blue Masson Trichrome stain with bright green color in Adobe Photoshop. The percentage of bright green pixels in each field was analyzed using Image-J.

### Terminal deoxynucleotidyl transferase dUTP nick end labeling staining

Paraffin-embedded tissue sections (5  $\mu$ m) were subjected to terminal deoxynucleotidyl transferase dUTP nick end labeling (TUNEL) using the DeadEnd Fluorometric TUNEL system (Promega, Madison, WI) according to the manufacturer's instructions. To mount and counterstain cells, Vectashield + 4',6-diamidino-2-phenylindole and Vectashield+ propidium iodide were diluted 1:400 into Vectashield mounting medium (Vector Laboratories, Burlingame, CA). For each sample, the numbers of bright green apoptotic nuclei were counted in 10 fields. Reported values are expressed as averages with SDs from 3–6 mice per treatment group.

### Bromodeoxyuridine staining

Two hours before euthanization, animals were injected with 50 mg/kg of bromodeoxyuridine (BrdU) in saline. Paraffin-embedded tissue sections (5  $\mu$ m) were subjected to BrdU staining using the Invitrogen BrdU staining kit (Invitrogen, Carlsbad, CA). The manufacturer's instructions were followed except in the antibody incubation step; for that step, slides were treated with biotinylated mouse anti-BrdU overnight at room temperature. For each sample, the numbers of BrdU positive cells were counted in 10 fields. Reported values are expressed as averages with SDs from 3–6 mice per treatment group.

### Statistical analysis

Specific tests used in each experiment are noted in the figure legends. All values shown are expressed as mean  $\pm$  SD. In experiments in which reported means represent multiple data sets from replicated experiments, statistical analysis was performed using the Student's two-way *t*-test, assuming homoscedasticity. In experiments in which reported means are from a single data set, statistical analysis was performed using one-way ANOVA followed by Tukey's honestly significant differences (HSD) test using the Vassar Stats website. Differences were considered significant when *P*-values were <0.05.

## RESULTS

We previously showed that treatment with NPC1 ASO decreased NPC1 expression specifically in the liver; knockdown was not observed in lung, brain, heart, spleen, or

kidneys. Liver knockdown of NPC1 caused mice to have hallmarks of NPC1 liver disease, including hepatomegaly, cholesterol storage, accumulation of lipid-laden cells, cell-death, inflammation, and fibrosis (10). To determine whether it is possible to recover from NPC1 liver disease, two treatment groups of mice were evaluated. One group was subjected to NPC1 knockdown for 9 weeks, representing a time point similar to one at which significant liver disease occurs in the NPC1<sup>nlh</sup> mouse model (9, 10, 21). The second group of mice was subjected to NPC1 knockdown for 15 weeks to determine the ability of the liver to recover from prolonged NPC1 liver disease. Treatment was halted after 9 or 15 weeks of NPC1 knockdown, and mice recovered for an additional 4, 9, or 15 weeks. As controls, NPC1 ASO-treated mice were compared with mice that had been treated with a mismatched ASO.

### NPC1 expression returns to normal levels by 9 weeks post-treatment

To quantify hepatic NPC1 protein expression, tissue samples were subjected to SDS-PAGE and Western blotting. Treatment with NPC1 ASO for 9 weeks reduced hepatic NPC1 protein expression to 15% of that in mismatched ASO-treated mice. Four weeks post-treatment, NPC1 protein expression returned to only about 40% of

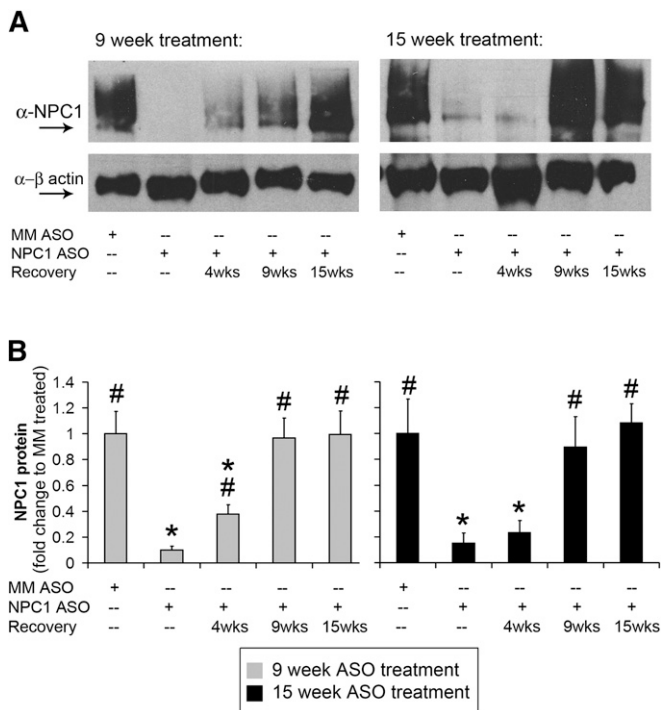


**Fig. 1.** NPC1 protein expression. A: Hepatic expression of NPC1 in mice treated with ASO for 9 weeks (left) or 15 weeks (right). Shown is a Western blot with representative samples for each treatment group. B: Densitometry analysis of NPC1 protein expression. Results are averages  $\pm$  SD of densitometry values for three independent Western blots, with three to six mice per treatment group. Values are expressed as the fold expression compared with mismatched treated mice. MM ASO, mismatched ASO. Comparisons were made using Student's two-tail *t*-test. #Significantly different from NPC1 ASO-treated mice, \*significantly different from MM ASO-treated mice.



that in mismatched ASO-treated mice. Nine weeks post-treatment, NPC1 protein expression returned to 100% of mismatched ASO-treated mice (Fig. 1 A, B, left).

Similarly, treatment with NPC1 ASO for 15 weeks decreased NPC1 expression to about 17% of that in mice treated with mismatched ASO; however, 4 weeks post-treatment, NPC1 protein expression recovered to only about 30% of that in mismatched ASO-treated mice. By 9 weeks post-treatment, NPC1 protein expression returned to 90% of mismatched ASO-treated mice (Fig. 1 A, B, right).

### Hepatosplenomegaly resolves after cessation of ASO treatment

NPC patients suffer from hepatosplenomegaly (1). NPC<sup>nih</sup> mice display hepatomegaly (9, 21), but there are no reports of splenomegaly. Splenomegaly does occur in the C57BLKS/J spm mouse model of NPC (22). We measured whole body, liver, and spleen weights (Fig. 2). NPC1 knock-down had no effect on body weight (Fig. 2A). However, treatment with NPC1 ASO for 9 and 15 weeks led to enlarged liver (Fig. 2B). Hepatosplenomegaly resolved by 4 weeks post-treatment, even though NPC1 protein levels were 40% and 30% of control levels, respectively. Although there were

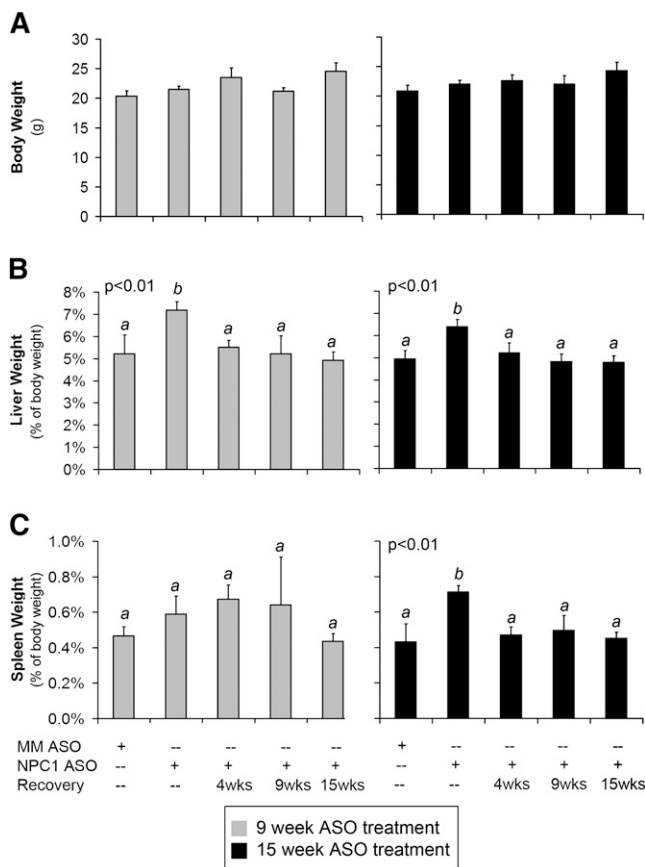


**Fig. 2.** Body, liver, and spleen weights. A: Body weight of mice treated with ASO for 9 weeks (left) or 15 weeks (right). B: Liver weight expressed as a percentage of body weight. C: Spleen weight expressed as a percentage of body weight. Results are averages  $\pm$  SD of values from three to six mice per group. Comparisons were made using ANOVA and Tukey's HSD test. Lettering (a, b) shows statistically dissimilar groups.

no changes in spleen size in 9 week treated mice, treatment with NPC1 ASO for 15 weeks led to splenomegaly, which resolved by 4 weeks post-treatment (Fig. 2C).

### Serum chemistries return to normal after halting ASO treatment

Serological profiling was performed to measure liver damage and liver function. The presence of alanine aminotransferase (ALT) in serum indicates that liver cells have lost integrity. In mice treated with NPC1 ASO for 9 or 15 weeks, serum ALT activity was increased (Fig. 3A). Serum

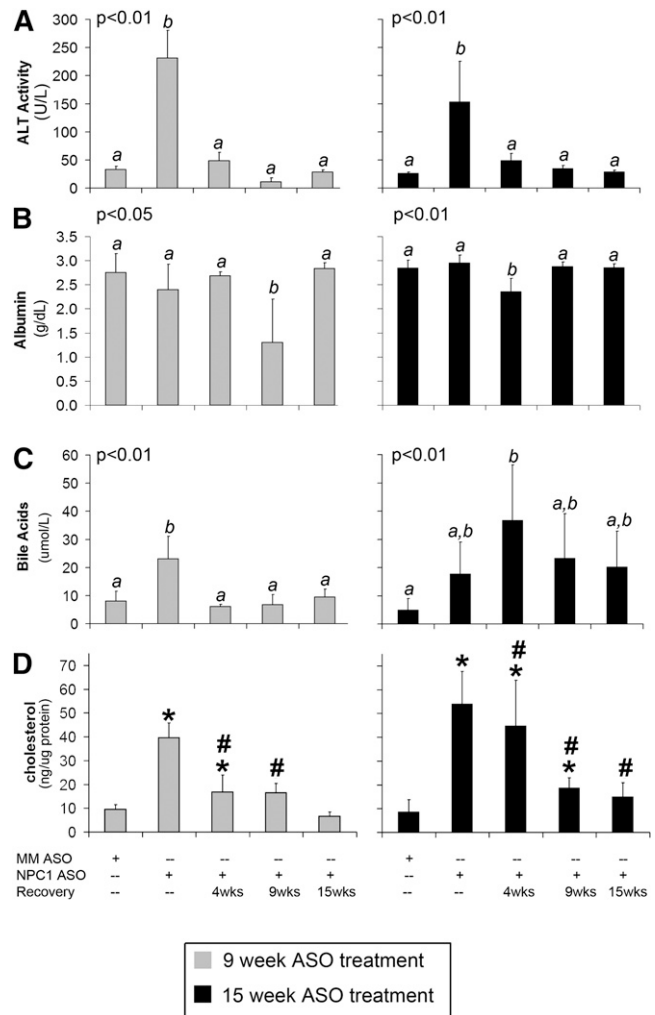
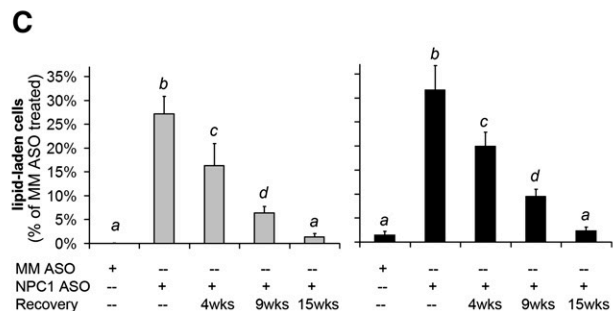
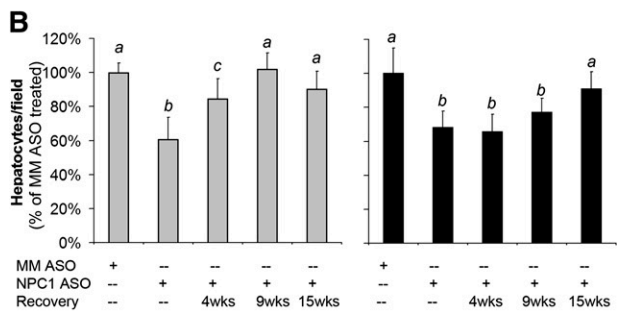
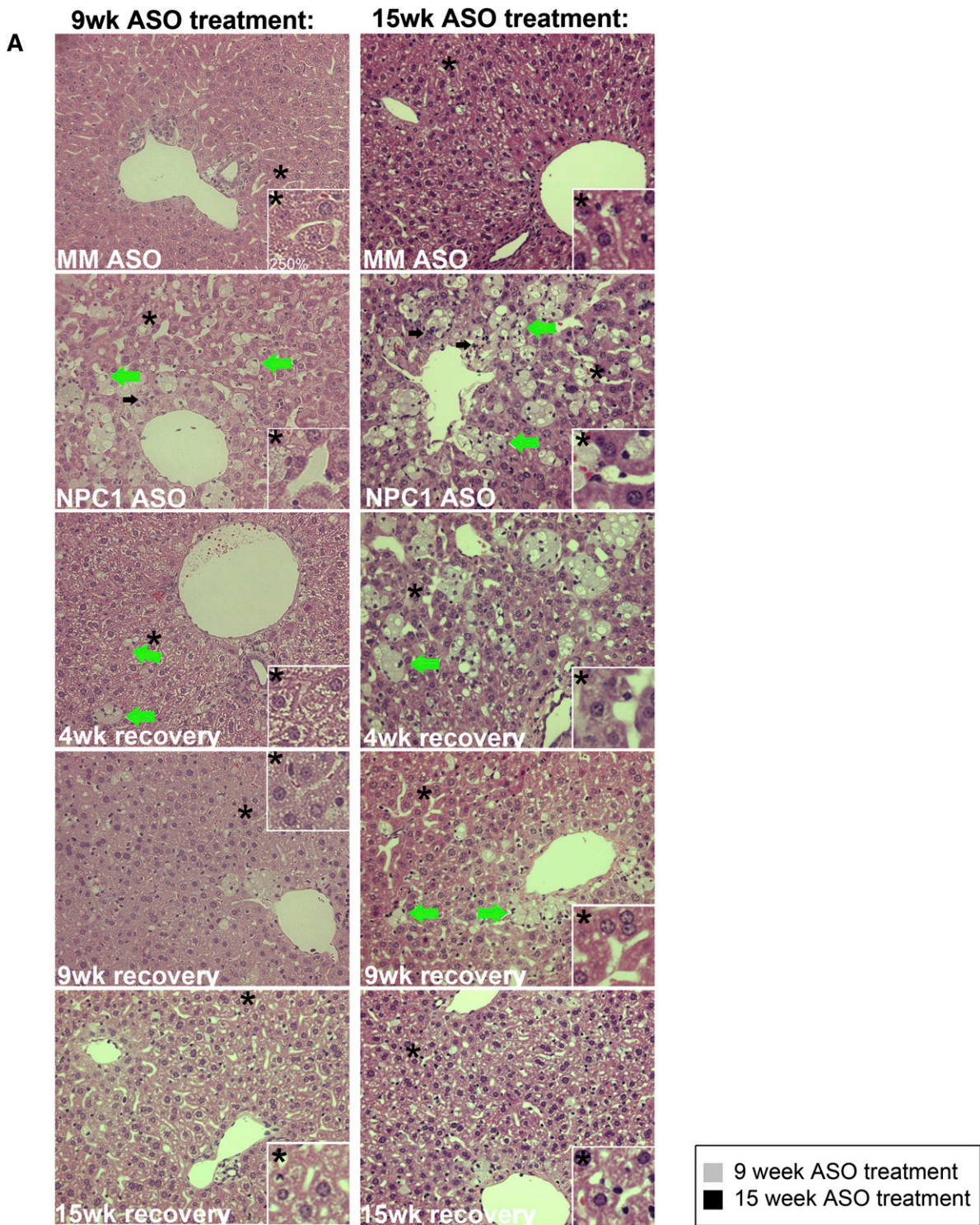


**Fig. 3.** Serological values and hepatic free cholesterol. A: ALT activity in serum of mice treated with ASO for 9 weeks (left) or 15 weeks (right). B: Albumin levels in serum. C: Bile acid levels in serum. Results shown are averages  $\pm$  SD of values from three to six mice per group. Comparisons for serological data were made using ANOVA and Tukey's HSD test. Lettering (a, b) shows statistically dissimilar groups. Samples with two letters represent values that are intermediate to the statistical groups and are thus not considered significantly different from either group. D: Hepatic free cholesterol content was measured as described in "Experimental procedures" and is expressed as ng/ $\mu$ g of protein. Cholesterol measurements are expressed as averages  $\pm$  SD from duplicate independent measurements with three to six mice per treatment group. Comparisons were made using Student's two-tail *t*-test. #Significantly different from NPC1 ASO-treated mice, \*significantly different from MM ASO-treated mice.





ALT activity decreased to the mismatched ASO-treated level by 4 weeks post-treatment in both 9 and 15 week treated mice.

To determine whether liver protein synthesis was affected, serum albumin levels were measured. As previously reported (10), serum albumin levels were unchanged after 9 or 15 weeks of treatment with NPC1 ASO (Fig. 3B). However, serum albumin levels dropped significantly in 9 week treated mice at 9 weeks after treatment, but then returned to normal (Fig. 3B, left). Similarly, mice treated for 15 weeks with NPC1 ASO had a drop in serum albumin at 4 weeks post-treatment that returned to normal by 9 weeks post treatment (Fig. 3B, right). Thus, both treatment groups of mice displayed a decrease in serum albumin levels 18–19 weeks after the onset of treatment, indicating that knockdown of NPC1 protein transiently affected liver protein synthesis.

Next, bile acid levels were measured. Nine week treatment with NPC1 ASO increased serum bile acids compared with mismatched ASO-treated mice, which resolved 4 weeks after cessation of ASO treatment (Fig. 3C, left). In contrast, increased bile acids caused by 15 week treatment remained significantly increased at 4 weeks post-treatment (Fig. 3C, right).

#### **Liver cholesterol storage resolves more quickly in 9 week NPC1 ASO-treated mice**

Increased serum bile acids could be caused by hepatocytes that were damaged from cholesterol storage due to NPC1 dysfunction. We expected NPC1 knockdown to cause hepatic cholesterol storage and that NPC1 reexpression would lead to resolution of cholesterol storage. We also hypothesized that cholesterol storage in livers would correlate with the presence of serum bile acids. To test for storage in livers, free and esterified cholesterol were extracted and quantified. Knockdown of NPC1 led to hepatic free cholesterol storage in both 9 and 15 week NPC1 ASO-treated mice (Fig. 3D). In 9 week treated mice, cholesterol levels resolved to those found in mismatched ASO-treated mice by 4 weeks post-treatment (Fig. 3D, left). Because bile acids remained high in serum from 15 week treated mice, we expected a slow resolution of hepatic cholesterol storage. In fact, cholesterol storage steadily reduced but did not resolve until 15 weeks post-treatment (Fig. 3D, right). We expected to observe an increase in cholesteryl esters, indicating movement of excess cholesterol from storage vesicles to lipid droplets. However, we were unable to measure significant differences in the amount of cholesteryl ester (not shown). A possible explanation is changes were not measurable within our level of resolution, or that cholesterol esters had been exported from the liver by the time point of measurement.

#### **Lipid-laden cell infiltration slowly resolves post-treatment**

Because serum liver enzymes returned to normal and cholesterol storage steadily resolved, we expected to find that the histological changes associated with NPC disease would improve. To determine how recovery from NPC1 knockdown affected liver tissue histology, H/E-stained tissue sections were examined. Mice lacking NPC1 had accumulation of lipid-laden macrophages in the liver, as shown previously (9–11, 23) (Fig. 4A, green arrows), accompanied by infiltration of liver parenchyma by immune cells (Fig. 4A, black arrows) and swelling of sinusoids (Fig. 4A, inset). The number of hepatocytes per field decreased to 60–70% of that in mismatched ASO-treated mice (Fig. 4B). During the recovery period, numbers of hepatocytes increased over time; in 9 week treated mice, hepatocytes returned to mismatched treated levels by 9 weeks after treatment (Fig. 4B, left). In 15 week treated mice, the number of hepatocytes per field returned more slowly to mismatched treated levels by 15 weeks after treatment (Fig. 4B, right).

Lipid-laden macrophages were counted and expressed as a percentage of the hepatocytes per field ratio. In both 9 and 15 week NPC1 ASO-treated mice, numbers of lipid-laden macrophages were approximately 30% of the hepatocytes per field; there were virtually no lipid-laden macrophages in mismatched ASO-treated mice. The numbers of lipid-laden macrophages steadily and significantly decreased post-treatment until returning to mismatched ASO-treated levels by 15 weeks post-treatment (Fig. 4C).

#### **Liver fibrosis does not resolve by 15 weeks post-treatment**

Liver injury leads to activation and proliferation of stellate cells, which produce extracellular matrix and cause fibrosis (24). Mice lacking NPC1 have liver fibrosis (9, 10) (Fig. 5A, white arrows). To determine whether halting NPC1 knockdown halts fibrosis, the amount of collagen deposition in parenchyma or around vessels was quantified in Masson's trichrome-stained tissue sections. Reexpression of NPC1 failed to stop fibrosis; indeed, fibrosis worsened in NPC1 ASO-treated livers over time. Nine week NPC1 ASO-treated mice showed increased parenchymal fibrosis 15 weeks post-treatment. Around vessels, fibrosis significantly increased by 9 weeks post-treatment (Fig. 5B, left). Mice treated for 15 weeks with NPC1 ASO had increased parenchymal fibrosis. Vessel fibrosis was also increased by 9 weeks post-treatment (Fig. 5B, right).

Collagen 1 $\alpha$ -2 mRNA expression was also tested using QPCR to measure fibrosis. In 9 week NPC1 ASO-treated mice, collagen mRNA expression increased to 6 times that of mismatched ASO-treated mice. After ceasing NPC1 knockdown, collagen expression steadily and significantly decreased over time until it returned to normal levels by 15 weeks after treatment (Fig. 5C, right). In 15 week NPC1

**Fig. 4.** H/E histology. A: H/E-stained sections of liver tissue in ASO-treated mice. Green arrow = lipid-laden macrophage. Black arrow = inflammatory cells. Inset = 250% magnification of area around asterisk. B: Quantification of the number of hepatocytes per field. For each treatment group, hepatocytes were counted in 10 independent fields. C: Quantification of lipid-laden macrophages. For each liver sample, 10 fields were quantified. Results shown are averages  $\pm$  SD of three to six mice per treatment group. Comparisons were made using ANOVA and Tukey's HSD test. Lettering (a, b) shows statistically dissimilar groups.

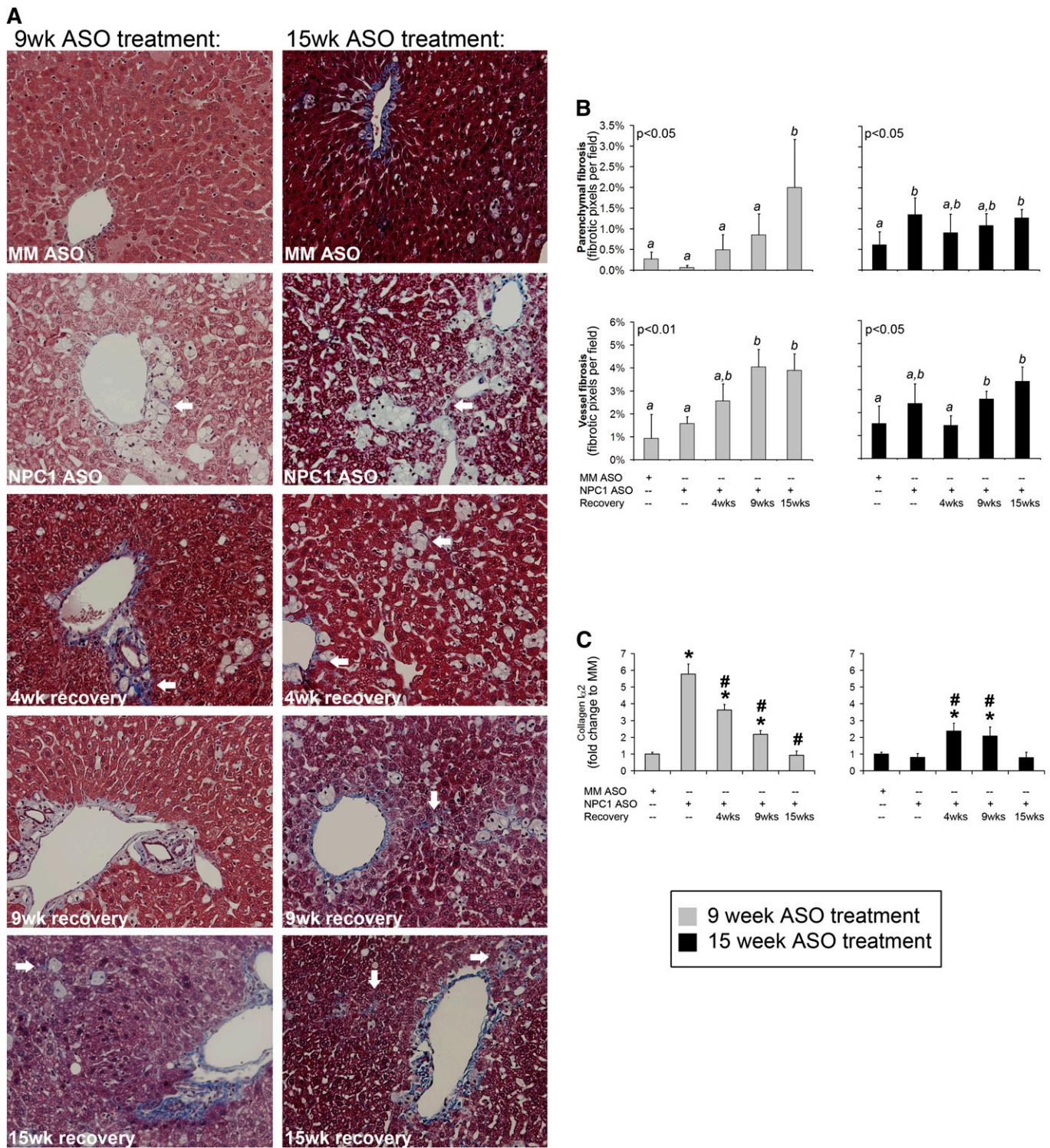


**Fig. 5.** Trichrome histology. A: Masson's trichrome stained sections of liver tissue in ASO-treated mice. White arrow = areas of blue-stained fibrosis. B: Quantification of parenchymal fibrosis (upper) and vessel fibrosis (lower) from trichrome stained tissue as described in "Experimental procedures." Results shown are averages  $\pm$  SD of three to six mice per treatment group. Comparisons were made using ANOVA and Tukey's HSD test. Lettering (a, b) shows statistically dissimilar groups. Samples with two letters represent values that are intermediate to the statistical groups and are thus not considered significantly different from either group. C: Expression of Collagen 1 $\alpha$ 2 mRNA as measured by QPCR is shown as fold difference compared with MM ASO-treated mice. Results are expressed as averages  $\pm$  SD from triplicate independent measurements from three to six mice per treatment group. Comparisons were made using Student's two tail *t*-test. #Significantly different from NPC1 ASO-treated mice, \*significantly different from MM ASO-treated mice.



ASO-treated mice, collagen mRNA expression failed to increase as dramatically as in 9 week treated mice. Collagen mRNA expression increased by approximately 2.5-fold at 4 and 9 weeks after halting NPC1 knockdown and returned to mismatched ASO-treated levels 15 weeks after halting NPC1 knockdown (Fig. 5C, left). Collagen mRNA expression was upregulated before fibrosis was perceived in the histology. This apparent delay in perceived fibrosis after collagen mRNA upregulation was likely due to the time it took for synthesis and export of collagen protein into the extracellular matrix where assembled collagen fibers are stained by Masson's trichrome.

### Cell death resolves along the same time line as cholesterol storage

NPC1 liver disease results in hepatocyte apoptosis and an inflammatory response (9, 10). The trigger for hepatocyte apoptosis in NPC disease is unknown; however, higher levels of liver apoptosis are correlated with increased lysosomal free cholesterol (23). We hypothesized that liver cell apoptosis is a consequence of lipid accumulation and so thus would remain elevated as long as excess free cholesterol is stored. To test whether cessation of NPC1 knockdown halts liver cell apoptosis, TUNEL staining of liver sections was used to count apoptotic nuclei (Fig. 6A). In mice treated for 9 weeks, cell death increased from approximately 0.5% of the ratio of hepatocytes per field in mismatched ASO-treated mice to approximately 2% of the ratio hepatocytes per field in NPC1 ASO-treated mice. This increase in cell death was comparable to previously reported values (10, 11). Four weeks post-treatment, liver cell apoptosis returned to mismatched ASO-treated levels (Fig. 6B, right); these results were consistent with our expectations, because cholesterol storage had significantly decreased by this time (Fig. 3D). In 15 week treated mice, liver cell death also significantly increased with NPC1 ASO treatment; however, liver cell death remained high 4 weeks post-treatment. Liver cell death resolved to mismatched ASO-treated levels by 9 weeks post-treatment (Fig. 6B, right). Again, these results were consistent with our expectations, because mice treated for 15 weeks with NPC1 ASO took more time to reduce stored free cholesterol (Fig. 3D).

### Liver cell proliferation increases post-treatment

Previously, we showed that NPC1 knockdown for 9 weeks led to cell proliferation. The majority of proliferative cells were hepatic stellate cells (10). However, the number of hepatocytes per field declined during NPC1 knockdown and returned to normal during the recovery phase (Fig. 4B), so we expected hepatocyte proliferation to increase during this time as well. To determine the effect of halting NPC1 knockdown on liver cell proliferation, we measured BrdU incorporation into proliferating cell nuclei using immunostaining. Figure 7 shows representative pictures from livers lacking proliferating cells (Fig. 7A) and livers containing proliferating cells (Fig. 7B, C). Consistent with our previous results (10), cell proliferation increased to approximately 10% of the hepatocytes

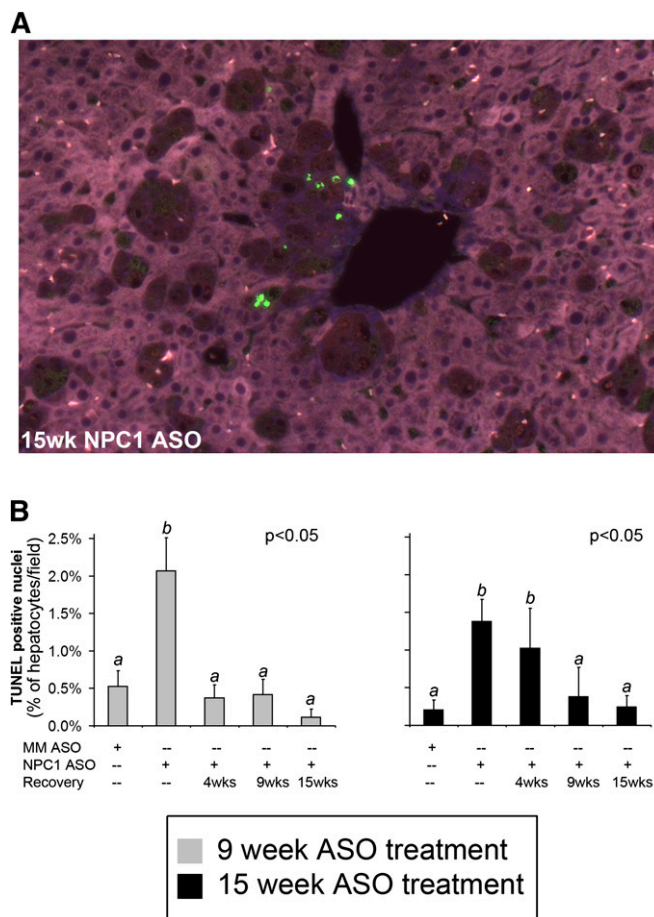


**Fig. 6.** Liver cell death. To measure cell death, liver sections were TUNEL stained as described in "Experimental procedures." A: Color merged picture of a liver section containing green TUNEL positive nuclei from a 15 week NPC1 ASO-treated mouse. The section was counter-stained with 4',6-diamidino-2-phenylindole and propidium iodide, appearing purple in the merged picture. B: Quantification of cell death as a percentage of the numbers of hepatocytes per field. For each sample, 10 fields were quantified. Results shown are averages  $\pm$  SD from quantification of three to six mice per treatment group. Comparisons were made using ANOVA and Tukey's HSD test. Lettering (a, b) shows statistically dissimilar groups. Samples with two letters represent values that are intermediate to the statistical groups and are thus not considered significantly different from either group.

per field ratio in 9 week NPC1 ASO-treated mice, whereas there were almost no proliferating cells in mismatched ASO-treated mice. Cell proliferation continued upon re-expression of NPC1, peaking at 9 weeks post-treatment (Fig. 7D, left). In 15 week treated mice, cellular proliferation also increased upon NPC1 reexpression 4 and 9 weeks post-treatment but returned to levels similar to mismatched ASO treated mice by 15 weeks post-treatment (Fig. 6D, right).

The morphology of most proliferating cells was consistent with that of stellate cells (Fig. 7B); however, we found that hepatocytes were also proliferating during the recovery phase. Figure 7C shows an example of proliferating hepatocytes. In both 9 and 15 week treated mice, hepatocyte proliferation increased after halting NPC1 knockdown



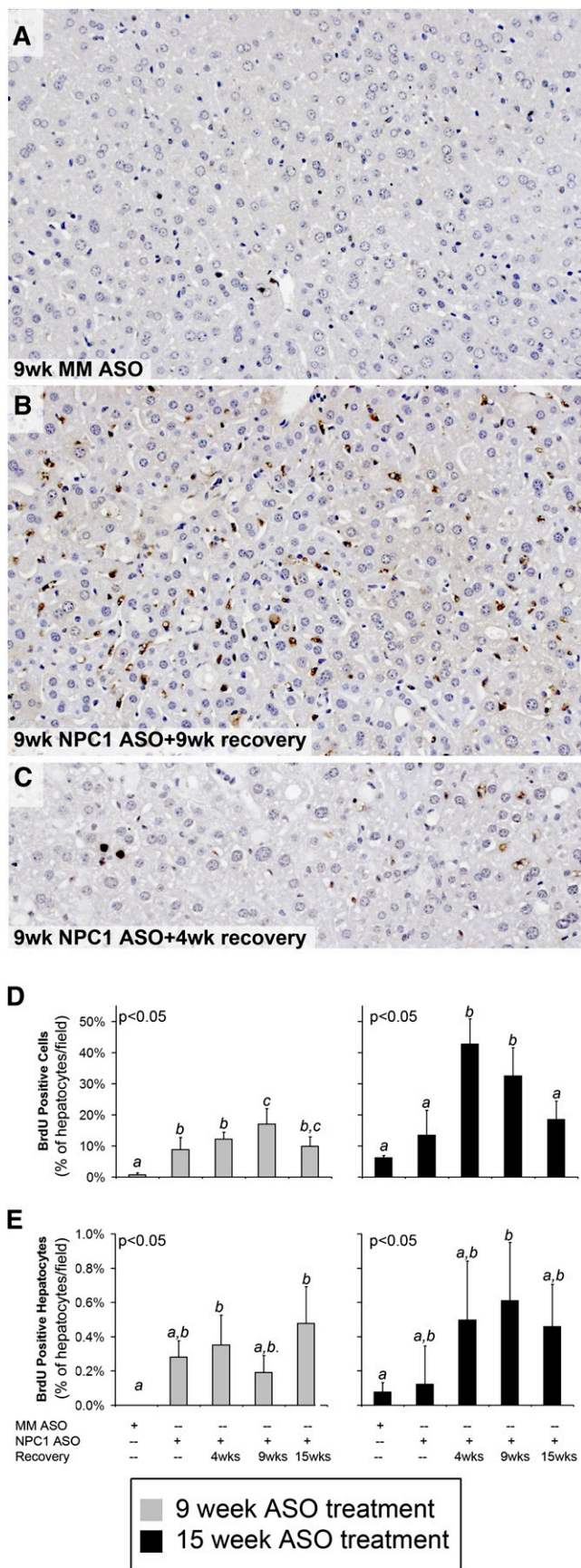


**Fig. 7.** Liver cell proliferation. To measure proliferation, liver sections were stained for BrdU incorporation as described in “Experimental procedures.” A: Representative liver section from a

(Fig. 7E). In 9 week treated mice, hepatocyte proliferation increased at 4 weeks post-NPC1 ASO treatment (Fig. 7E, left). In 15 week treated mice, hepatocyte proliferation increased at a later time, at 9 weeks post-treatment (Fig. 7E, right).

### Hepatic cholesterol homeostasis gene expression is affected by recovery

Finally, we examined the mechanisms that regulate cholesterol homeostasis. One regulator, SREBP2, is a cholesterol-responsive transcription factor that upregulates expression of genes containing sterol responsive elements. Sterol responsive element-containing genes include those important for cholesterol biosynthesis, such as 3-hydroxy-3-methylglutaryl (HMG)-CoA Reductase, as well as SREBP2 itself (25).

Previous reports have shown that the SREBP2 pathway is upregulated in NPC1<sup>mh</sup> mouse livers (9, 21). Increased cholesterol biosynthesis in NPC disease models is likely due to the fact that cholesterol is sequestered within the endocytic system and thus is not transported to the endoplasmic reticulum to inhibit the activation of SREBP2. QPCR was used to determine whether expression of SREBP2-regulated genes was altered post-ASO treatment. Similar to previously reported results in the NPC1 ASO mouse model (10), knockdown of NPC1 for 9 weeks increased SREBP2 expression 2-fold compared with mismatched ASO-treated mice. Additionally, SREBP2 expression remained upregulated at 4 and 9 weeks post-treatment but was resolved by 15 weeks (Fig. 8A, left). In contrast, mice treated for 15 weeks with NPC1 ASO had decreased SREBP2 mRNA expression to 0.1-fold of mismatched ASO-treated mice, which then significantly increased to 4- to 6-fold of mismatched ASO-treated mice in the recovery time points (Fig. 8A, right). HMG-CoA reductase expression was unchanged in 9 week treated mice for all time points. However, in 15 week treated mice, HMG-CoA reductase expression significantly increased 6-fold in the post-treatment time points (Fig. 8B).

A second important cholesterol homeostatic regulatory mechanism involves nuclear receptor activation of genes involved in cholesterol efflux. The LXR/retinoid X receptor heterodimer is an example of a nuclear receptor that is important in cholesterol homeostasis. Many genes

9 week MM ASO-treated mouse, which has no proliferating cells. B: Representative liver section from a 9 week NPC1 ASO + 9 week recovery-treated mouse showing many proliferating cells with a dark brown reaction product. C: Representative liver section from a 9 week NPC1 ASO + 4 week recovery-treated mouse in showing proliferating hepatocytes. D: Quantification of total proliferating hepatocytes as a percentage of the numbers of hepatocytes per field. E: Quantification of proliferating hepatocytes as a percentage of the numbers of hepatocytes per field. For each sample, 10 fields were quantified. Results shown are averages  $\pm$  SD of three to six mice per treatment group. Comparisons were made using ANOVA and Tukey’s HSD test. Lettering (a, b) shows statistically dissimilar groups. Samples with two letters represent values that are intermediate to the statistical groups and are thus not considered significantly different from either group.

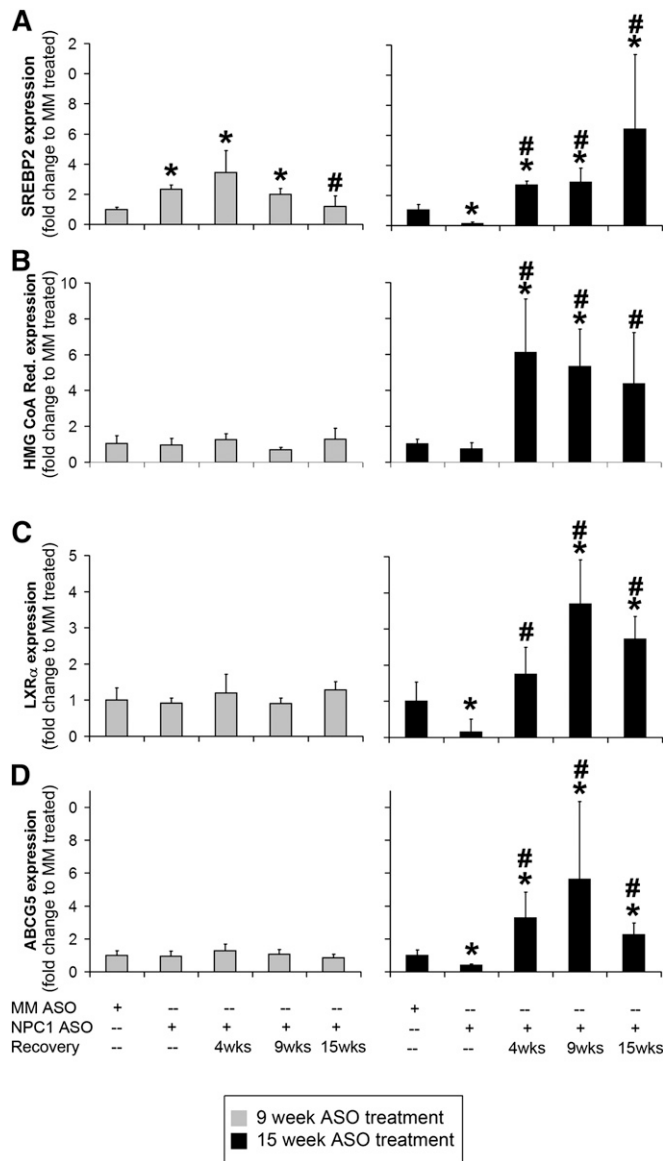


**Fig. 8.** Cholesterol homeostasis. Expression of SREBP2 (A), HMG-CoA reductase (B), LXR $\alpha$  (C), and ABCG5 (D) mRNA as measured by QPCR is shown as fold difference compared with MM ASO-treated mice. QPCR results are expressed as averages  $\pm$  SD from triplicate independent measurements with three to six mice per treatment group. Comparisons were made using Student's two-tail *t*-test. #Significantly different from NPC1 ASO-treated mice, \*significantly different from MM ASO-treated mice.

activated by LXR/retinoid X receptor are important for cholesterol efflux, such as ABCG5, which moves cholesterol from the liver into bile (26). The effect of hepatic NPC1 knockdown and recovery on the expression of LXR-regulated gene expression was tested. Nine week NPC1 ASO treatment did not change LXR $\alpha$  mRNA expression or that of the LXR target ABCG5 (Fig. 8C, D, left) These results are consistent with our previous report (10). In contrast, 15 week NPC1 ASO-treated mice displayed decreased LXR $\alpha$  and ABCG5 expression compared with mismatched ASO-treated mice. Post-treatment, expression of LXR $\alpha$  and ABCG5 significantly increased for 4, 9, and 15 weeks (Fig. 8C, D, right).

Treating mice with an *npc1*-specific ASO leads to a unique mouse model that is suited to understanding the ability of the liver to heal from NPC disease. This model has two important features. First, the knockdown is liver specific, and the only phenotype mice exhibit are classic signs of NPC liver disease: hepatomegaly, hepatic free cholesterol storage, elevated serum liver enzymes, and formation of foamy vacuolated macrophages. Hepatic apoptosis is increased accompanied by stellate cell activation and fibrosis (10).

Second, as shown in this study, NPC1 knockdown is reversible. Cessation of treatment results in a slow, steady reappearance of NPC1 protein. This allows us to examine the consequences of NPC1 reexpression in the liver, which is not possible in any other NPC mouse model at this time.

Here, we show that significant recovery occurs in the liver, even when expression of NPC1 is below normal; such results are encouraging, because they show that a therapy does not have to restore full activity of NPC1 to be beneficial. In mice treated for 9 weeks with NPC1 ASO that were allowed to recover without treatment for 4 weeks, NPC1 protein had increased to 40% of control levels. At that point, hepatic cholesterol content, serum liver enzymes and bile acid, and the number of apoptotic cells had returned to control levels. It took more time for lipid-laden macrophages to clear. Cell proliferation was high throughout the recovery phase.


The average age that NPC patients are diagnosed is about 10 years (2); however, it takes an average of 4 years to diagnose NPC in patients that clinically present with hepatosplenomegaly or jaundice (27). Patients typically die from NPC during adolescence (1). Rarely are patients diagnosed before tissue damage occurs; in fact, most patients would not be treated before liver damage or neurodegeneration is discovered. Thus, we chose to understand liver recovery in mice at a time when liver disease exists (9 weeks) and when liver disease is prolonged (15 weeks). Our results emphasize that early diagnosis of NPC will be important in achieving any beneficial outcome from potential therapeutics. Mice treated with NPC1 ASO for 15 weeks showed splenomegaly and had a slower resolution of hepatic cholesterol storage and apoptosis. Four weeks post-treatment, when NPC1 protein was about 30% of control levels, cholesterol storage had only slightly decreased and serum bile acids were still increasing. Only hepatomegaly and serum ALT had returned to normal. This suggests that serum ALT may be a good first indication that the liver is recovering, but serum bile acid level is a better indication of full recovery.

We were surprised to find that, in both treatment groups, fibrosis increased within the parenchyma and around vessels during the recovery periods. Stellate cells are responsible for deposition of collagen (24), and we see prolonged proliferation of liver cells with morphology consistent to stellate cells. The apparent proliferation of hepatic stellate cells may be the result of ongoing inflammation, as stellate



also plays a role in inflammatory processes in the liver (28). No treatments have been found that decrease fibrosis once it has occurred; instead, it may be beneficial to prevent collagen deposition and fibrosis in the first place.

The cholesterol homeostatic phenotype in 15 week treated mice is concerning. First, cholesterol storage does not resolve as quickly in these mice. The slow resolution of cholesterol storage likely accounts for the similar slow resolution of hepatic cell death. Why cholesterol storage remains elevated 4 weeks post-treatment is not as explainable. The cholesterol homeostasis mechanisms have never been published for a mouse with NPC liver disease at this age because NPC<sup>mh</sup> mice do not survive so long, but we did not expect increased SREBP-2 mRNA levels. Reversal after long-term knockdown also led to increased mRNA levels for HMG-CoA reductase, the rate-limiting enzyme in cholesterol biosynthesis, as well as LXR $\alpha$  and ABCG5, which are involved in cholesterol efflux. We do not know if there are commensurate changes in protein levels. If so, the increased biosynthesis could explain the delayed reduction of liver cholesterol storage, and increased export could explain continuing high levels of serum bile acids. The changes in homeostatic gene expression may represent a response to exacerbated liver damage and inflammation, as is seen in nonalcoholic fatty liver disease. Notably, inflammatory stress has been shown to increase expression of SREBP2 mRNA and low density lipoprotein receptor in apolipoprotein E knockout mice (29); similarly, increased SREBP2 expression was observed in liver samples from patients with non-alcoholic fatty liver disease (30). It should be noted, however, that neither of these studies showed increased expression of genes implicated in cholesterol efflux, such as LXR $\alpha$  (29) or ABCG8 (30). Further investigation into the cholesterol homeostatic phenotype of mice with prolonged NPC1 knockdown in the liver is warranted.

Although the liver is capable of recovery from NPC disease, we do not yet know how well the nervous system can recover. This is especially important, because most NPC patients die due to neurological disease complications. Despite this, measuring recovery in the liver as a model for therapeutic efficacy of drugs for NPC is worth considering, because therapeutic benefit can be measured without the confounding issue of a drug passing through the blood-brain barrier to a target. 

The authors thank Melanie Vincent, Hiroko Nagase, and Kristen Myers for their technical assistance. The authors also thank Maribel Rios for the use of her microscope.

## REFERENCES

- Patterson, M. C., M. T. Vanier, K. Suzuki, J. A. Morris, E. Carstea, E. B. Neufeld, J. E. Blanchette-Mackie, and P. G. Pentchev. 2001. Niemann-Pick Disease Type C: a lipid trafficking disorder. *In* The Metabolic and Molecular Bases of Inherited Disease. C. R. Scriver, A. L. Beaudet, W. S. Sly, and D. Valle, editors. McGraw-Hill, New York. 3611–3633.
- Garver, W. S., G. A. Francis, D. Jelinek, G. Shepherd, J. Flynn, G. Castro, C. Walsh Vockley, D. L. Coppock, K. M. Pettit, R. A. Heidenreich, et al. 2007. The National Niemann-Pick C1 disease database: report of clinical features and health problems. *Am. J. Med. Genet. A*. **143A**: 1204–1211.
- Reif, S., Z. Spirer, G. Messer, M. Baratz, B. Bembi, and Y. Bujanover. 1994. Severe failure to thrive and liver dysfunction as the main manifestations of a new variant of Niemann-Pick disease. *Clin. Pediatr. (Phila.)*. **33**: 628–630.
- Putterman, C., J. Zelingher, and D. Shouval. 1992. Liver failure and the sea-blue histiocyte/adult Niemann-Pick disease. Case report and review of the literature. *J. Clin. Gastroenterol.* **15**: 146–149.
- Rutledge, J. C. 1989. Progressive neonatal liver failure due to type C Niemann-Pick disease. *Pediatr. Pathol.* **9**: 779–784.
- Dumontel, C., C. Girod, F. Dijoud, Y. Dumez, and M. T. Vanier. 1993. Fetal Niemann-Pick disease type C: ultrastructural and lipid findings in liver and spleen. *Virchows Arch. A Pathol. Anat. Histopathol.* **422**: 253–259.
- Yerushalmi, B., R. J. Sokol, M. R. Narkewicz, D. Smith, J. W. Ashmead, and D. A. Wenger. 2002. Niemann-pick disease type C in neonatal cholestasis at a North American Center. *J. Pediatr. Gastroenterol. Nutr.* **35**: 44–50.
- Kelly, D. A., B. Portmann, A. P. Mowat, S. Sherlock, and B. D. Lake. 1993. Niemann-Pick disease type C: diagnosis and outcome in children, with particular reference to liver disease. *J. Pediatr.* **123**: 242–247.
- Beltray, E. P., J. A. Richardson, J. D. Horton, S. D. Turley, and J. M. Dietschy. 2005. Cholesterol accumulation and liver cell death in mice with Niemann-Pick type C disease. *Hepatology*. **42**: 886–893.
- Rimkunas, V. M., M. J. Graham, R. M. Crooke, and L. Liscum. 2008. In vivo antisense oligonucleotide reduction of NPC1 expression as a novel mouse model for Niemann Pick type C-associated liver disease. *Hepatology*. **47**: 1504–1512.
- Rimkunas, V. M., M. J. Graham, R. M. Crooke, and L. Liscum. 2009. TNF- $\alpha$  plays a role in hepatocyte apoptosis in Niemann-Pick type C liver disease. *J. Lipid Res.* **50**: 327–333.
- Fausto, N. 2001. Liver regeneration. *In* The Liver Biology and Pathobiology. I. Arias, J. Boyer, F. Chisari, N. Fausto, and D. Schachter, editors. Lippincott Williams & Wilkins, Philadelphia, PA. 591–610.
- Geary, R. S., T. A. Watanabe, L. Truong, S. Freier, E. A. Lesnik, N. B. Sioufi, H. Sasmor, M. Manoharan, and A. A. Levin. 2001. Pharmacokinetic properties of 2'-O-(2-methoxyethyl)-modified oligonucleotide analogs in rats. *J. Pharmacol. Exp. Ther.* **296**: 890–897.
- Crooke, R. M., M. J. Graham, K. M. Lemonidis, C. P. Whipple, S. Koo, and R. J. Perera. 2005. An apolipoprotein B antisense oligonucleotide lowers LDL cholesterol in hyperlipidemic mice without causing hepatic steatosis. *J. Lipid Res.* **46**: 872–884.
- Yamaguchi, K., L. Yang, S. McCall, J. Huang, X. X. Yu, S. K. Pandey, S. Bhanot, B. P. Monia, Y. X. Li, and A. M. Diehl. 2008. Diacylglycerol acyltransferase I anti-sense oligonucleotides reduce hepatic fibrosis in mice with nonalcoholic steatohepatitis. *Hepatology*. **47**: 625–635.
- Liu, B., S. D. Turley, D. K. Burns, A. M. Miller, J. J. Repa, and J. M. Dietschy. 2009. Reversal of defective lysosomal transport in NPC disease ameliorates liver dysfunction and neurodegeneration in the npc1<sup>-/-</sup> mouse. *Proc. Natl. Acad. Sci. USA*. **106**: 2377–2382.
- Repa, J. J., S. D. Turley, G. Quan, and J. M. Dietschy. 2005. Delineation of molecular changes in intrahepatic cholesterol metabolism resulting from diminished cholesterol absorption. *J. Lipid Res.* **46**: 779–789.
- Repa, J. J., H. Li, T. C. Frank-Cannon, M. A. Valasek, S. D. Turley, M. G. Tansey, and J. M. Dietschy. 2007. Liver X receptor activation enhances cholesterol loss from the brain, decreases neuroinflammation, and increases survival of the NPC1 mouse. *J. Neurosci.* **27**: 14470–14480.
- Folch, J., M. Lees, and G. H. S. Stanley. 1957. A simple method for the isolation and purification of total lipids from animal tissues. *J. Biol. Chem.* **226**: 497–509.
- Liscum, L., and G. J. Collins. 1991. Characterization of Chinese hamster ovary cells that are resistant to 3-b-[2-(diethylamino) ethoxy] androst-5-en-17-one inhibition of low density lipoprotein-derived cholesterol metabolism. *J. Biol. Chem.* **266**: 16599–16606.
- Garver, W. S., D. Jelinek, J. N. Oyarzo, J. Flynn, M. Zuckerman, K. Krishnan, B. H. Chung, and R. A. Heidenreich. 2007. Characterization of liver disease and lipid metabolism in the Niemann-Pick C1 mouse. *J. Cell. Biochem.* **101**: 498–516.
- Miyawaki, S., S. Mitsuoka, T. Sakiyama, and T. Kitagawa. 1982. Sphingomyelinosis, a new mutation in the mouse: a model of Niemann-Pick disease in humans. *J. Hered.* **73**: 257–263.
- Beltray, E. P., B. Liu, J. M. Dietschy, and S. D. Turley. 2007. Lysosomal unesterified cholesterol content correlates with liver

- cell death in murine Niemann-Pick type C disease. *J. Lipid Res.* **48**: 869–881.
24. Rojkind, M. G. P., 2001. Pathophysiology of liver fibrosis. In *The Liver Biology and Pathobiology*. I. Arias, J. Boyer, F. Chisari, N. Fausto, and D. Schachter, editors. Lippincott Williams & Wilkins: Philadelphia, PA. 721–738.
25. Soccio, R. E., and J. L. Breslow. 2004. Intracellular cholesterol transport. *Arterioscler. Thromb. Vasc. Biol.* **24**: 1150–1160.
26. Fievet, C., and B. Staels. 2009. Liver X receptor modulators: effects on lipid metabolism and potential use in the treatment of atherosclerosis. *Biochem. Pharmacol.* **77**: 1316–1327.
27. Yanjanin, N.M., J. I. Velez, A. Gropman, K. King, S. E. Bianconi, S. K. Conley, C. C. Brewer, B. Solomon, W. J. Pavan, M. Arcos-Burgos, et al. 2010. Linear clinical progression, independent of age of onset, in Niemann-Pick disease, type C. *Am J Med Genet B Neuropsychiatr Genet.* **153B**: 132–140.
28. Atzori, L., G. Poli, and A. Perra. 2009. Hepatic stellate cell: a star cell in the liver. *Int. J. Biochem. Cell Biol.* **41**: 1639–1642.
29. Ma, K. L., X. Z. Ruan, S. H. Powis, Y. Chen, J. F. Moorhead, and Z. Varghese. 2008. Inflammatory stress exacerbates lipid accumulation in hepatic cells and fatty livers of apolipoprotein E knockout mice. *Hepatology.* **48**: 770–781.
30. Caballero, F., A. Fernandez, A. M. De Lacy, J. C. Fernandez-Checa, J. Caballeria, and C. Garcia-Ruiz. 2009. Enhanced free cholesterol, SREBP-2 and StAR expression in human NASH. *J. Hepatol.* **50**: 789–796.